Viscoelastic Behavior in Toluene at High Pressure

R. G. REIN, JR.,[1] C. M. SLIEPCEVICH, and S. E. BABB
University of Oklahoma, Norman, Okla.

The torsionally oscillating quartz crystal viscometer was used to obtain Newtonian viscosity-pressure data for isopentane, *n*-octane, and methylcyclohexane at pressures up to 8000 atm. for comparison with the Bridgman's data. Values for the complex viscosity and shear modulus were then obtained for toluene. Toluene exhibits viscoelastic behavior at pressures above about 3000 atm. when a 60-kc. crystal is used. By the method of reduced variables the measurements for toluene were converted to atmospheric pressure to obtain a shear relaxation spectrum, from which it is apparent that viscoelastic behavior occurs in toluene for shear rates greater than 5×10^6 sec^{-1}.

ALTHOUGH the viscoelastic behavior of liquids with complex molecules is well known, it is less commonly observed in fluids with structurally simple molecules. However, viscoelastic behavior can be expected at high shear rates even in structurally simple fluids (*2, 9*). In this study the viscoelastic behavior of toluene was investigated at high pressure with a quartz crystal viscometer. By use of the method of reduced variables, results obtained with this viscometer at a single frequency but different pressures were converted to an equivalent series of higher frequencies at atmospheric pressure. Because angular frequency ($\omega = 2\pi f$) is assumed to be equal to shear rate, measurements at the resultant higher frequencies were equivalent to measurements at the higher shear rates necessary to observe viscoelasticity in toluene.

EQUIPMENT AND PROCEDURE

The techniques involved in using the crystal viscometer have been elaborated (*1, 10, 13, 14*). In brief, the components of the complex viscosity of a fluid ($\eta^* = \eta_1 - i\eta_2$), or the components of the complex shear modulus ($G^* = G_1 + iG_2 = i\omega\eta^*$), are related to the mechanical impedance, $Z_M = R_M + iX_M$, of the oscillating rod immersed in the fluid by (*11*)

$$\eta_1 = G_2/\omega = 2X_M R_M/\omega\rho \quad (1)$$

and

$$\eta_2 = G_1/\omega = (R_M^2 - X_M^2)/\omega\rho \quad (2)$$

where ρ is the fluid density and $\omega = 2\pi f$ is the angular frequency of the crystal, which is assumed to equal the shear rate. The components of the mechanical impedance are related to the measured resonant frequency, f, of the crystal in a given fluid at a given pressure and to the crystal resistance, R_E, at the resonance in the given fluid at the given pressure by (*10*)

$$R_M = (R_E - R_{E_0})/K_r \quad (3)$$

and

$$X_M = (f_0 - f)/K_f \quad (4)$$

where X_M is the mechanical reactance of the crystal, K_r and K_f are crystal constants obtained from calibration in Newtonian fluids of known viscosity and density, and subscript o refers to values obtained in an inviscid fluid (such as air at 1-atm. pressure). Previous investigators have concluded that both K_r and K_f are essentially independent of pressure (*1*).

Figure 1 indicates the electrical components used in this investigation to measure the resonant frequency of the crystal and the crystal resistance at resonance. The resonant frequency of the crystal used in this particular investigation was near 60 kc. The oscillator used was a Hewlett-Packard Model 200CD, the frequency counter was a Hewlett-Packard Model 521G, and the detector was a General Radio 1232-A null detector which had a sensitivity of 6 μv. at full scale deflection at 60 kc.

For the measurements at high pressure the crystal was mounted in the high pressure cell. A schematic diagram of the high pressure equipment is shown in Figure 2.

After the crystal had been mounted in the high pressure cell and prior to pressurization, calibration data were obtained at 1 atm. with Newtonian fluids (air, *n*-octane, carbon tetrachloride, lubricating oils, and NBS viscosity standards) of known density and viscosity.

Following calibration, the resonant frequency and resistance at resonance were measured at elevated pressures for isopentane, *n*-octane, toluene, and methylcyclohexane. These measurements were used to determine the viscous and elastic behavior of the fluids at elevated pressures.

After the cell had been filled with the desired fluid, preliminary pressurization of the cell was obtained after isolating the air pump and hand pump designated "high pressure" in Figure 2. Sufficient fluid could be pumped into the cell with the hand pump designated "low pressure" to bring the pressure in the cell to about 1 katm. (1000 atm.). After the necessary measurements of resonant fre-

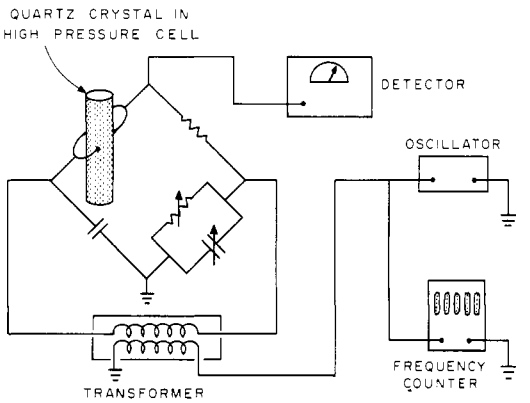

Figure 1. Electrical components used in determining resonant frequency and resistance

[1] Present address, University of Oklahoma Research Institute, Norman, Okla.

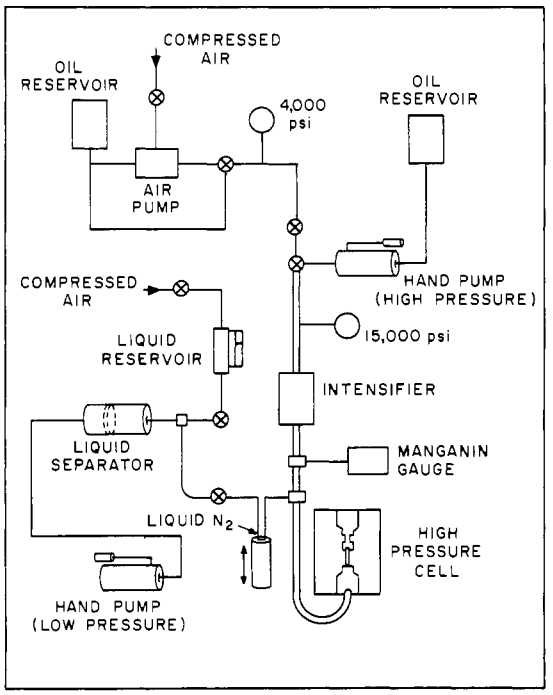

Figure 2. High pressure flow diagram

quency and resistance at resonance were obtained in the pressure range 1 atm. to 1 katm., the low pressure end of the system was isolated by freezing the liquid in the appropriate line with liquid nitrogen. Following isolation of the low pressure end of the system, pressure in the cell could be increased by driving the intensifier piston down with the air pump or "high pressure" hand pump, after which pressure could be decreased by driving the piston back up with the pressure of the liquid in the cell.

The crystal resonant frequency and resistance at resonance were measured at constant pressure after pressure had been both increased and decreased. When measurements taken at a given pressure, obtained by increasing the pressure, did not agree with measurements taken at the same pressure but obtained by decreasing pressure, or vice versa, the pressure was cycled to determine if a hysteresis effect existed. If a hysteresis effect did exist, it was usually an indication of a bad electrical connection to the crystal or a short of the electrical leads. In this event the crystal was removed from the cell, the electrical malfunction was corrected, and the procedure was repeated.

After the necessary data were obtained with one liquid, that liquid was removed from the cell, and the cell was cleaned with petroleum ether. The cell was cleaned without removing the crystal from the cell, which eliminated the need for replacing the seals and recalibrating the crystal. Following removal of the solvent from the cell, the cell was put under a vacuum for several hours, then filled with the next fluid to be investigated, and the high pressure measurements were repeated.

RESULTS AND CALCULATIONS

To calculate η_1, η_2, G_1, or G_2 for each fluid from the frequency and resistance data it is necessary to know the fluid density as a function of pressure. Bridgman's compressibility data (*4*) were used to obtain the density of isopentane and *n*-octane as functions of pressure at the temperature of the measurements. The concept of the average fluid (*6*) was used to extend the range of methylcyclohexane compressibility data (*5*). Published values of the compressibility of toluene were available over the entire pressure range (*7*). It is estimated that all density values are accurate to $\pm 2\%$.

Estimates were made of the expected error in the measured values of the resonant frequency and resistance at resonance (*13*), thus determining upper and lower limits for R_M and X_M. The estimated error in resistance measurements was about $\pm 6\%$ except for a few measurements at R_E greater than 1 megohm, for which the error was $\pm 20\%$. The estimated frequency error is also a function of R_E and varies from 0 c.p.s. at low resistances to ± 5 c.p.s. when $R_E > 1$ megohm. For all measurements except those in toluene above about 3000 atm. the upper limit of X_M overlapped with the lower limit of R_M; thus it is possible that $R_M = X_M$ within the limits of experimental precision except at noted for toluene. (If $R_M = X_M$, viscoelastic behavior does not exist according to Equation 2.)

If $R_M = X_M$, Equation 1 may be written;

$$\eta_1 = G_2/\omega = 2R_M^2/\omega\rho \qquad (1a)$$

Equation 1a was used to calculate η_1 for all data except those on toluene where $R_M > X_M$. Equation 1a is preferable to Equation 1 because R_M is more sensitive to viscosity changes than X_M.

Viscosity values calculated according to Equation 1a reproduced Bridgman's viscosity-pressure data (*3*) for all fluids within the limits of experimental precision. Figure 3 gives a representative comparison.

For measurements in toluene with the 60-kc. crystal at the higher pressures the lower limits of R_M were consistently higher than the upper limits of X_M and therefore $\eta_2 = G_1/\omega$ was greater than zero. Because the reduced frequency (directly proportional to shear rate) will be in the region where viscoelastic behavior is observed, measurements with a 20-kc. crystal in toluene at the highest pressure (7.37

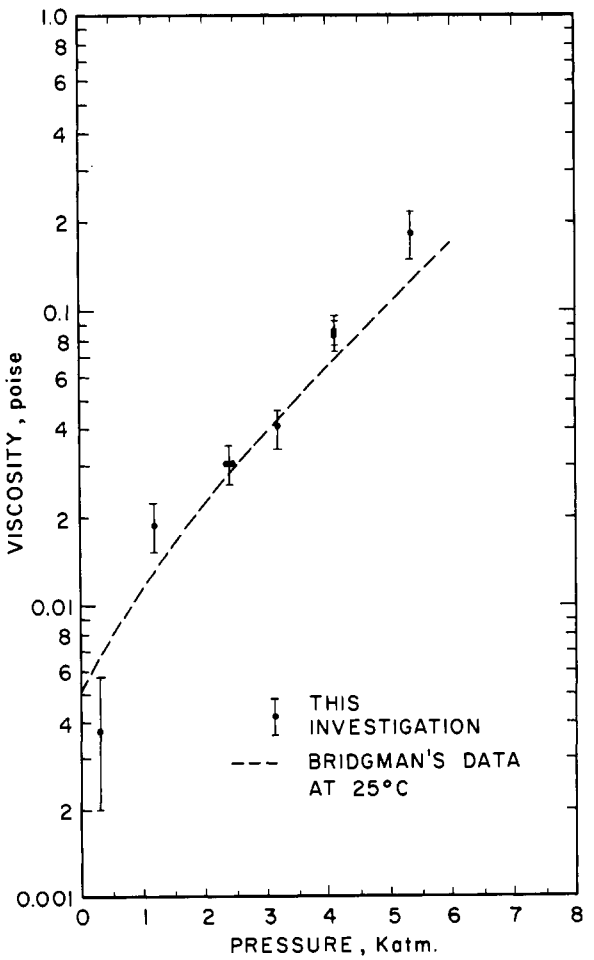

Figure 3. Effect of pressure on viscosity of n-octane at 25° C.

katm.) would also be expected to indicate viscoelastic behavior. However, viscoelasticity could not be confirmed with a 20-kc. crystal because of lower precision in the experimental measurements at this particular pressure for toluene. The upper limits in the values of X_M overlapped the lower limits of the values of R_M, obscuring the expected viscoelastic effect.

For the 60-kc. crystal the upper and lower limits of η_1, G_2, η_2, and G_1 at the various pressures were calculated of reduced variables (*1, 11*), values of G_1, G_2, and η_1 obtained at various pressures were converted to atmospheric pressure in order to determine the frequency behavior of G_1, G_2, and η_1 atmospheric pressure. The reduced variables are defined as follows (*1, 11, 12*):

$$f_r = a_{TP} f \tag{5}$$

$$a_{TP} = (T_0/T)\,(\rho_0/\rho)\,(\eta_T/\eta_0)_P(\eta_P/\eta_0)_T \tag{6}$$

$$G_{1r} = G_1(T_0\rho_0/T\rho) \tag{7}$$

$$G_{2r} = G_2(T_0\rho_0/T\rho) \tag{8}$$

$$\eta_{1r} = \eta_1(\eta_0/\eta_T)_P(\phi_0/\eta_P)_T \tag{9}$$

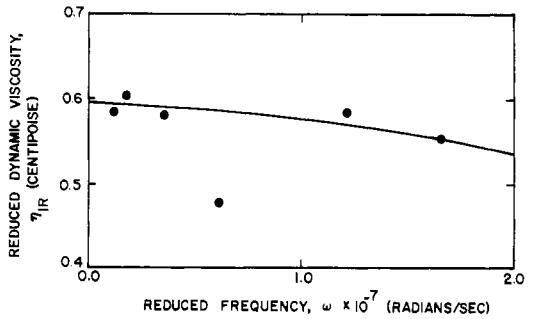

Figure 4. Real part of the complex viscosity, η_{1r}, as a function of angular frequency in reduced variables

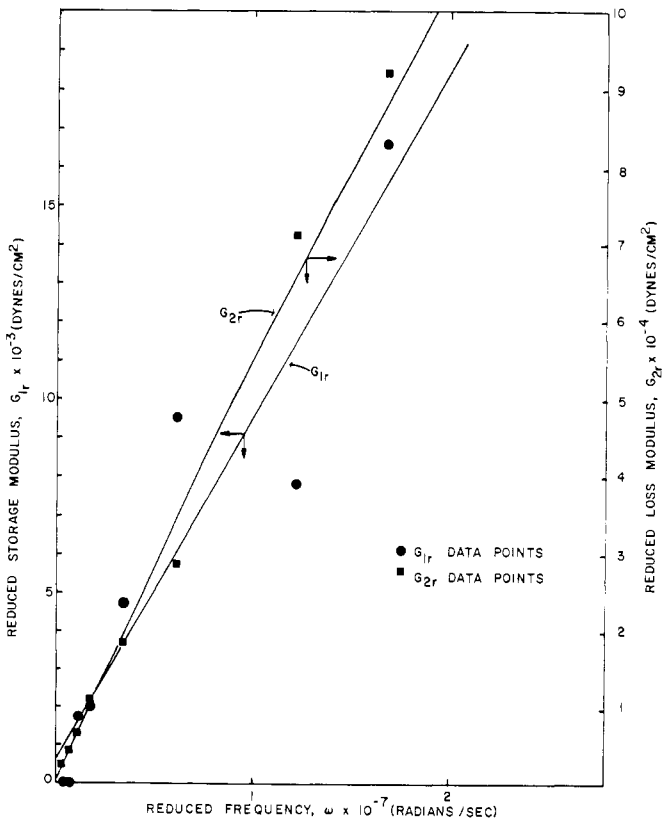

Figure 5. Reduced components of the complex shear modulus as functions of reduced angular frequency

The maximum deviation in η_{1r} and G_{2r} values (obtained from use of the appropriate upper and lower limits of R_M and X_M in Equations 1 and 2) is $\pm 12\%$. The maximum deviation in G_{1r}, $\pm 33\%$, is much greater because the calculations involve differences of numbers of the same magnitude.

Figures 4 and 5 show the reduced parameters, η_{1r}, G_{1r}, and G_{2r} as functions of reduced angular frequency. The values of these parameters at 4.0×10^5 and 7.1×10^5 radians per second represent values of the appropriate parameter if there is no viscoelastic behavior. At these and lower frequencies the limits of R_M and X_M overlapped and viscoelastic behavior is not probable, as previously explained. Therefore, inclusion of data points corresponding to nonviscoelastic behavior at these frequencies is justified.

The change in η_{1r} with reduced frequency shown in Figure 4 is indicative of the behavior expected at the onset of viscoelasticity. The reason for the departure of the experimental point at a reduced frequency of 6×10^6 radians per second is unexplained.

Different types of least squares curves were tried in order to fit the data of G_{1r} and G_{2r} as functions of frequency. The smooth curves shown in Figure 5 are the least squares curves that give the best correlation consistent with the precision of the data. The curves are $G_{1r} = (8.94 \times 10^{-4})\omega$ with a correlation coefficient of 0.93, and $G_{2r} = (8.48 \times 10^{-4})\omega^{0.972}$ with a correlation coefficient of 1.00.

These curves of G_{1r} and of G_{2r} as functions of frequency were used to obtain independent representations of the shear relaxation spectrum, H, as a function of relaxation time, τ, for toluene. H is given in terms of the imaginary (Im) and real (Re) parts of G_{1r} and G_{2r}, respectively (*8*):

$$H[\text{at } \tau = 1/\omega] = (2/\pi)\ \text{Im}\ G_{1r}[\text{ at } \omega e^{\pm i\pi/2}] \tag{10}$$

$$H[\text{at } \tau = 1/\omega] = 1/\omega] = (2/\pi)\ \text{Re}\ G_{2r}[\text{at } \omega e^{\pm i\pi/2}] \tag{11}$$

Curves for the relaxation spectrum calculated from G_{1r} and G_{2r} data are shown in Figure 6.

As expected, independent calculations of the relaxation spectrum for toluene by Equation 10 or 11 both approach

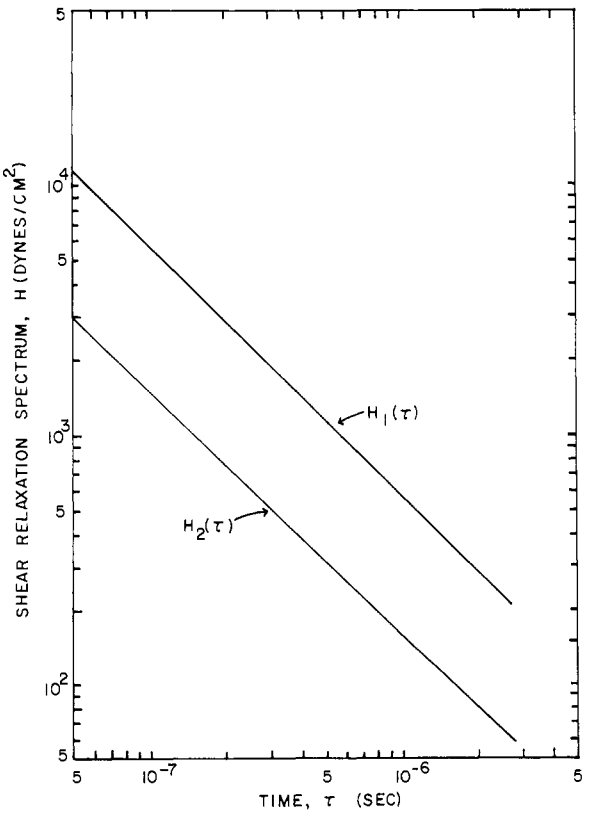

Figure 6. Initial part of shear relaxation spectrum for toluene

zero at long times, as shown in Figure 6. In addition, the relaxation spectra calculated from G_{1r} and G_{2r} data show qualitative agreement with each other, in that both curves have the same shape (a linear relation between log H and log τ). However, since the magnitudes of the spectra are different, quantitative conclusions are less reliable. The quantitative difference in the curves is understandable considering errors inherent in calculating G_{1r} from experimental data obtained in this study compared to errors in calculating G_{2r}.

ACKNOWLEDGMENT

G. J. Scott's assistance throughout the experimental phase of the work is appreciated.

LITERATURE CITED

(1) Appeldoorn, J. K., Okrent, E. H., Philippoff, W., *Proc. Am. Petrol. Inst.* (III) **42**, 163 (1962).
(2) Barlow, A. J., Lamb, J., *Proc. Roy. Soc.* **A253**, 52 (1952).
(3) Bridgman, P. W., *Proc. Am. Acad. Arts Sci.* **61**, 57 (1926).
(4) *Ibid.*, **66**, 185 (1931).
(5) *Ibid.*, **77**, 189 (1949).
(6) Bridgman, P. W., "The Physics of High Pressure," p. 131, G. Bell and Sons, London, 1952.
(7) Chang, Z. T., *Chinese J. Phys.* **1**, 1 (1934).
(8) Ferry, J. D., "Viscoelastic Properties of Polymers," p. 53, Wiley, New York, 1961.
(9) Fredrickson, A. G., "Principles and Applications of Rheology," pp. 122, 150, Prentice-Hall, Englewood Cliffs, N.J., 1964.
(10) Mason, W. P., *Trans. Am. Soc. Mechan. Engrs.* **69**, 359 (1949).
(11) Philippoff, W., in "Physical Acoustics," W. P. Mason, ed., Vol. II, Part B, p. 35, Academic Press, New York, 1965.
(12) *Ibid.*, p. 42.
(13) Rein, R.G., Jr., Ph.D. thesis, University of Oklahoma, Norman, Okla., 1967.
(14) Rouse, P.E., Jr., Bailey, E.D., Minkin, J.A., *Proc. Am. Petrol. Inst.* **30M** (III), 54 (1950).

RECEIVED for review October 16, 1967. Accepted June 4, 1968. Financial support provided by Autoclave Engineers, Inc., and the National Science Foundation, Grant GK857.

Energy of Combustion and Differential Thermograms of Organic Azides

G. C. DENAULT, P. C. MARX, and H. H. TAKIMOTO
Aerospace Corp., El Segundo, Calif. 90243

The heats of formation of two series of triazoles, 3-azido-s-triazoles, I, and 4-amino-3-azido-s-triazoles, II, are reported from the heats of combustion in an oxygen bomb calorimeter. Differential thermograms were also obtained to determine the thermal stability of each compound.

THE ENERGY CONTENT of a chemical compound is of major importance in the evaluation of its potential as a propellant ingredient. As a part of a program to synthesize and measure physical properties of energetic compounds, the heats of combustion and formation of two series of triazoles, 3-azido-*s*-triazoles, I, and 4-amino-3-azido-*s*-triazoles, II, were determined. Differential thermograms were also obtained on these compounds to determine their thermal stability.

Although the heats of combustion of few organic azides (*1, 2, 6*) have been described, the energy contents of high nitrogen heterocyclic azides have not been reported. The paucity of such information is undoubtedly due to the difficulty in synthesis and the ease with which these compounds decompose during the purification process. The problem of synthesis has been circumvented by the initial preparation of the hydrazinotriazoles and their subsequent conversion to the corresponding azidotriazoles.

EXPERIMENTAL

Materials. The 3-azido-*s*-triazoles, I, and 4-amino-3-azido-*s*-triazoles, II, were prepared by treatment of the corresponding 4-amino-3-hydrazino-*s*-triazole hydrochlorides (*3, 8, 9*) with 2 and 1 equivalents of nitrous acid, respectively. The azides prepared in this manner are listed in Table I. A representative example for each is given below.

3-AZIDO-*s*-TRIAZOLES. A solution of 8.9 grams of sodium nitrite in 15 ml. of water was added dropwise to an ice-cold solution of 9.0 grams of 4-amino-3-hydrazino-*s*-triazole hydrochloride in 65 ml. of 2*N* hydrochloric acid. When half of the nitrite had been added, a precipitate appeared

Table I. Azido-s-triazoles[a]

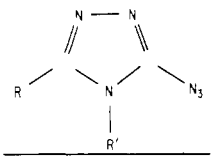

No.	R	R′	M.P., °C.[b]	Formula	Carbon, % Calcd.	Carbon, % Found	Hydrogen, % Calcd.	Hydrogen, % Found	Nitrogen, % Calcd.	Nitrogen, % Found
Ia	H	H	120–21.5	$C_2H_2N_6$[c]	21.82	21.60	1.83	2.40	76.34	76.35
Ib	CH_3	H	143–45	$C_3H_4N_6$	29.03	29.18	3.25	3.46	67.72	67.57
Ic	C_2H_5	H	116.5–19	$C_4H_6N_6$	34.78	34.74	4.38	4.62	60.84	60.85
Id	C_6H_5	H	191–92 dec.	$C_8H_6N_6$	51.61	51.69	3.25	3.44	45.14	45.36
IIa	H	NH_2	52–55 dec.	$C_2H_3N_7$	19.20	18.82	2.42	2.59	78.38	78.38
IIb	CH_3	NH_2	84–86 dec.	$C_3H_5N_7$	25.90	25.78	3.63	3.90	70.48	70.31
IIc	C_2H_5	NH_2	81–83 dec.	$C_4H_7N_7$	31.37	31.61	4.61	4.89	64.02	64.06
IId	C_6H_5	NH_2	150–51 dec.	$C_8H_7N_7$	47.75	47.71	3.51	3.52	48.73	48.72

[a] Analyses performed in this laboratory. [b] All melting points uncorrected. [c] Samples detonated, breaking combustion tubes during analyses, and good values for hydrogen could not be obtained.